A cross-sectional comparison of brain glucose and ketone metabolism in cognitively healthy older adults, mild cognitive impairment and early Alzheimer's disease

E. Croteau [a,b], C.A. Castellano [a], M. Fortier [a], C. Bocti [a,c], T. Fulop [a,c], N. Paquet [d,e], S.C. Cunnane [a,b,c,*]

[a] Research Center on Aging, Université de Sherbrooke, Sherbrooke, Canada
[b] Department of Pharmacology & Physiology, Université de Sherbrooke, Sherbrooke, Canada
[c] Department of Medicine, Université de Sherbrooke, Sherbrooke, Canada
[d] Departments of Nuclear Medicine, Université de Sherbrooke, Sherbrooke, Canada
[e] CHUS Research Center, Université de Sherbrooke, Sherbrooke, Canada

ARTICLE INFO

ABSTRACT

Introduction: Deteriorating brain glucose metabolism precedes the clinical onset of Alzheimer's disease (AD) and appears to contribute to its etiology. Ketone bodies, mainly β-hydroxybutyrate and acetoacetate, are the primary alternative brain fuel to glucose. Some reports suggest that brain ketone metabolism is unchanged in AD but, to our knowledge, no such data are available for MCI.
Objective: To compare brain energy metabolism (glucose and acetoacetate) and some brain morphological characteristics in cognitively healthy older adult controls (CTL), mild cognitive impairment (MCI) and early AD.
Methods: 24 CTL, 20 MCI and 19 AD of similar age and metabolic phenotype underwent a dual-tracer PET and MRI protocol. The uptake rate constants and cerebral metabolic rate of glucose (K_{Glu}, CMR_{Glu}) and acetoacetate (K_{AcAc}, CMR_{AcAc}) were evaluated with PET using [18F]-fluorodeoxyglucose ([18F]-FDG), a glucose analogue, and [11C]-acetoacetate ([11C]-AcAc), a ketone PET tracer. Regional brain volume and cortical thickness were evaluated by T1-weighted MRI.
Results: In AD compared to CTL, CMR_{Glu} was ~11% lower in the frontal, parietal, temporal lobes and in the cingulate gyrus ($p < 0.05$). K_{Glu} was ~15% lower in these same regions and also in subcortical regions. In MCI compared to CTL, ~7% glucose hypometabolism was present in the cingulate gyrus. Neither regional nor whole brain CMR_{AcAc} or K_{AcAc} were significantly different between CTL and MCI or AD. Reduced gray matter volume and cortical thinning were widespread in AD compared to CTL, whereas, in MCI compared to CTL, volumes were reduced only in the temporal cortex and cortical thinning was most apparent in temporal and cingulate regions.
Discussion: This quantitative kinetic PET and MRI imaging protocol for brain glucose and acetoacetate metabolism confirms that the brain undergoes structural atrophy and lower brain energy metabolism in MCI and AD and demonstrates that the deterioration in brain energy metabolism is specific to glucose. These results suggest that a ketogenic intervention to increase energy availability for the brain is warranted in an attempt to delay further cognitive decline by compensating for the brain glucose deficit in MCI and AD.

1. Introduction

Regional brain glucose hypometabolism is one of the hallmarks of Alzheimer's disease (AD) (Brown et al., 2014). [18F]-Fluoro-deoxyglucose (FDG), a glucose analogue and radiotracer for positron emission tomography (PET) studies, has been extensively studied to assess the magnitude and progression of impaired brain glucose uptake in AD (Brown et al., 2014; Cunnane et al., 2016a). Like other groups, we have used PET-[18F]-FDG and reported the now classical regional brain glucose hypometabolism pattern in mild AD (Castellano et al., 2015; Castellano et al., 2017; Cunnane et al., 2016a; Dukart et al., 2013; Mosconi et al., 2009).

Ketones (β-hydroxybutyrate and acetoacetate), are the brain's primary alternative fuel when plasma glucose is decreased. In prolonged starvation, ketones can supply up to 80% of adult human brain energy requirements (Cahill, 2006). Brain ketone utilization is directly proportional to blood ketone level over a wide blood ketone concentration range (Courchesne-Loyer et al., 2016; Nugent et al., 2014). Using the PET ketone tracer, ^{11}C-acetoacetate (AcAc), we have reported that

Table 1
Characteristics of the cognitively healthy older controls (CTL) and patients with mild cognitive impairment (MCI) or early Alzheimer disease (AD).

	CTL (n = 24)	MCI (n = 20)	AD (n = 19)
Age (y)	72.8 ± 5.8	76.9 ± 5.8	73.1 ± 4.8
Gender (M/F)	10/15	9/12	8/11
Mini-mental state examination (score/30)	29.4 ± 0.9	27.5 ± 2.0*	25.5 ± 2.4*
Body mass index	26.7 ± 3.8	26.5 ± 3.1	24.3 ± 2.9
Glucose (mM)	5.2 ± 0.5	5. ± 0.4	5.4 ± 0.6
Hemoglobin A1c (%)	5.8 ± 0.3	5.6 ± 0.5	5.9 ± 0.4
Acetoacetate (mM)	0.12 ± 0.08	0.14 ± 0.05	0.11 ± 0.07
β-hydroxybutyrate (mM)	0.25 ± 0.18	0.25 ± 0.12	0.21 ± 0.16

* One-way ANOVA and Tukey's post hoc test $p < 0.05$.

brain metabolism of ketones is unchanged in early AD (Castellano et al., 2015; Castellano et al., 2017; Cunnane et al., 2016a). Our results confirm earlier reports that used the arterio-venous difference method and showed that brain ketone uptake is still normal in moderately advanced AD (Lying-Tunell et al., 1981; Ogawa et al., 1996).

Mild cognitive impairment (MCI) is the prodromal state to AD (Gauthier et al., 2006). Objective evidence of cognitive decline is present in MCI but it does not yet interfere with the activities of daily living. Impaired glucose metabolism is also present in certain brain regions in MCI (Jicha et al., 2008; Pagani et al., 2015) but whether brain ketone uptake is altered in MCI has not been reported.

The primary aim of the present study was to compare brain ketone and glucose consumption in a cross-sectional study of age-matched cognitively healthy older adults, MCI and AD. Our secondary aim was to assess the presence of brain atrophy and thinning of the brain cortex in these three groups.

2. Material and methods

2.1. Participants

This study was approved by the institutional review board and ethics committees (Health and Social Services Center, Sherbrooke University Geriatrics Institute and the Centre hospitalier universitaire de Sherbrooke) and written informed consent was obtained for all participants. Participants underwent a pre-screening visit including medical history questionnaire and blood analysis. Exclusion criteria included smoking, substance abuse, and untreated/uncontrolled hypertension, dyslipidemia or diabetes. Cognitively healthy older adults (CTL, $n = 24$) had a Mini-Mental State Examination (MMSE) score of ≥27/30. Criteria for inclusion in the MCI group ($n = 20$) were: subjective memory complaint, score below the normative normal score for age in one or more cognitive domains (typically including episodic memory, language and executive function), intact score of activities of daily living (score ≤ 15/24 at the IADL subscale of the Functional Autonomy Measuring System; (Hebert et al., 1988)), plus no evidence of AD or depression (score ≤ 10 on the Geriatric Depression Scale 30-items). (Petersen, 2004). Probable or possible AD ($n = 19$) was defined using the National Institute on Aging - Alzheimer's Association (NIA-AA) criteria (Castellano et al., 2017; McKhann et al., 2011) with or without use of prescribed medication for AD.

2.2. PET and MRI neuroimaging protocols

After a light breakfast, participants fasted for about 6 h before starting the imaging session. All participants underwent a 3D T1-weighted MRI at 1.5 or 3 T (Pfefferbaum et al., 2012). The protocol for the 1.5 T MRI scans (Sonata, Siemens Medical Solutions, Erlangen, Germany) was as follows:
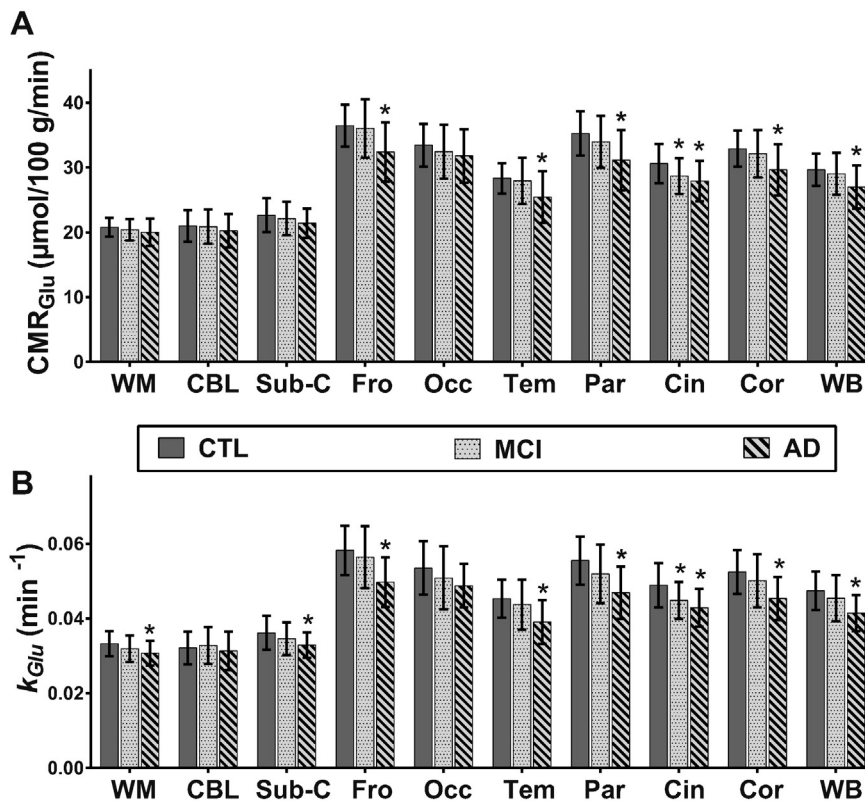

Fig. 1. Regional and whole brain glucose (^{18}F–flurodeoxyglucose) uptake in healthy older controls (CTL; $n = 24$), mild cognitive impairment (MCI; $n = 20$) and early Alzheimer's disease (AD; $n = 19$). **A:** Regional cerebral metabolic rate of glucose per unit of brain tissue (CMR$_{Glu}$). **B:** Regional constant rate uptake (K_{Glu}). WM; white-matter, CBL; cerebellum, Sub-C; sub-cortical region (thalamus, caudate, putamen, pallidum, hippocampus, amygdala and accumbens), Fro; frontal, Occ; occipital, Tem; temporal, Par; parietal, Cin; cingulate, Cor; cortex, WB; whole brain. Data are presented as mean ± SD; * $p < 0.05$, one way ANOVA with post-hoc Tukey tests.

scan duration = 9.14 min, TR = 16.0 ms, TE = 4.7 ms, field of view = 256 × 240 × 192 mm, flip angle = 20°, voxel size = 1 mm^3 isotropic, denoising = non-local means filter. The protocol for the 3 T MRI scan (Ingenia, Philips Healthcare, Best, The Netherlands) was as follows: scan duration = 6 min, TR = 7.9 ms, TE = 3.5 ms, field of view = 240 × 240 × 150, flip angle = 8° and 1 mm isotropic voxels.

For all participants, brain PET acquisitions were obtained on a PET/CT (Gemini TF, Philips Healthcare, Eindhoven, The Netherlands) with a field of view of 25 cm and axial field of 18 cm. Data were acquired in dynamic list mode with an isotropic voxel size of 2 mm^3. Catheters were placed in both forearms for tracer injection and blood sampling, respectively. Arterialization of venous forearm blood was achieved by wrapping the hand with a heating pad set at 44 °C. To calibrate the input function, blood sampling was performed throughout the PET scan which lasted 10 min for [^{11}C]-AcAc and 60 min for [^{18}F]-FDG. First, 370 MBq of [^{11}C]-AcAc was administrated for a total scan duration of 10 min with time frames of 12 × 10 s, 8 × 30 s, and 1 × 4 min, and blood samples taken at 3, 6, and 8 min post-injection. An hour later, 185 MBq of [^{18}F]-FDG was administered in a quiet environment with dim lights. [^{18}F]-FDG acquisition was started at 30 min post-injection and lasted for 30 min with time frames of 6 × 5 min. Blood samples were obtained at 8, 16, 32.5, 42.5, 52.5 and 57.5 min post-injection. Plasma samples were counted in a gamma counter (Cobra, Packard, United States) and cross-calibrated to the PET image. Plasma glucose and ketones were measured using an automated clinical chemistry analyzer (Dimension Xpand Plus; Siemens Healthcare Diagnostics, Deerfield, IL, USA) using commercial glucose assay (Siemens Healthcare Diagnostics, Deerfield, IL, USA) and previously described ketones assays (Courchesne-Loyer et al., 2013).

2.3. PET and MRI image analysis

The dynamic PET acquisitions were analysed as previously described (Nugent et al., 2014), with the exception of a reduced duration of the [^{18}F]-FDG scan (30–60 min, instead of 0–60 min post-tracer infusion). The Patlak method was used to quantify the brain uptake rate constants and the cerebral metabolic rates for [^{18}F]-FDG (K_{Glu} and CMR$_{Glu}$) and [^{11}C]-AcAc (K_{AcAc} and CMR$_{AcAc}$), respectively (Logan, 2000). PET and MR images were co-registered and CMR (expressed as μmol/100 g/min) was calculated using the following equation:

$$CMR = K \times Cp/LC \qquad [1]$$

where K represents the uptake rate constant of the radiotracers (min^{-1}), C_p the plasma arterial concentration of the tracer and lumped constant (LC) (1.0 for [^{11}C]-AcAc and 0.8 for [^{18}F]-FDG). The input functions derived from each brain image were partial volume-corrected and calibrated against the corrected radioactivity in blood samples obtained during each PET scan (Nugent et al., 2014). For [^{18}F]-FDG, the first part of the time-activity curve was modeled by a linear function to reflect the increasing blood [^{18}F]-FDG concentration during the automated injection of the tracer. The initial linear function, blood-sampled and image-derived input functions were concatenated and interpolated through a tri-exponential decay fit (PMOD 3.7 Technologies Ltd., Zurich, Switzerland) (Vriens et al., 2009). The estimated cerebral ketone consumption (AcAc plus β-hydroxybutyrate combined or CMR$_{Ketone}$) was analysed as previously described (Blomqvist et al., 1995; Castellano et al., 2017). CMR was also expressed by region and by percentage/region of gray matter.
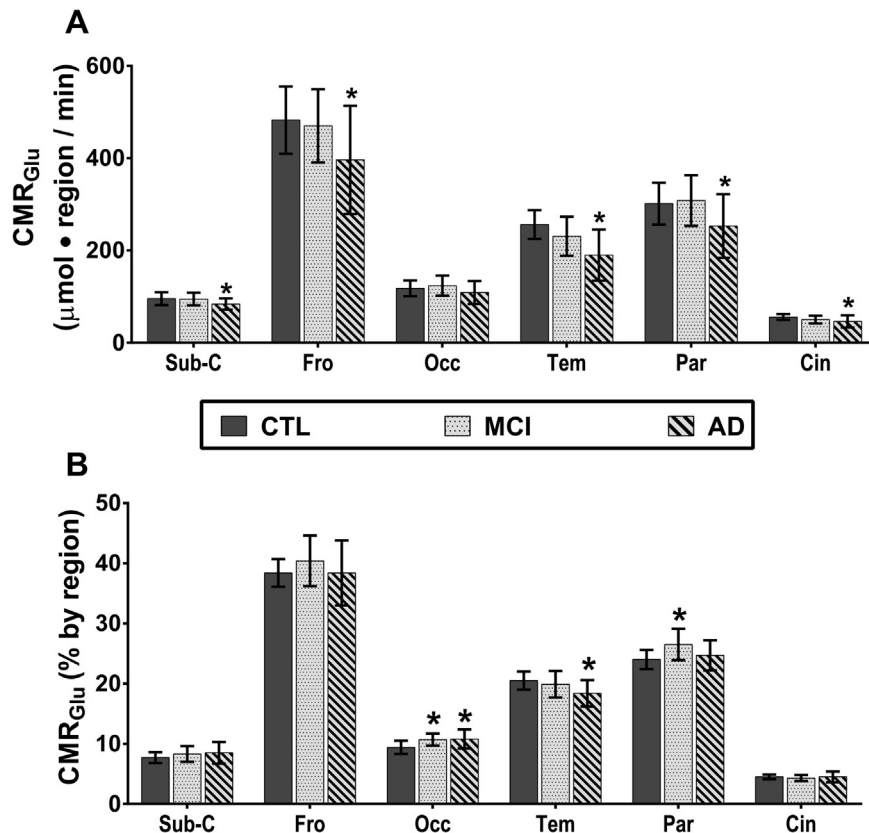

Fig. 2. Regional (^{18}F-flurodeoxyglucose) uptake in healthy older controls (CTL; $n = 24$), mild cognitive impairment (MCI; $n = 20$) and early Alzheimer's disease (AD; $n = 19$). **A**: Cerebral metabolic rate of glucose (CMR$_{Glu}$) by major anatomical brain region. **B**: Percentage CMR$_{Glu}$ by region. Sub-C; sub-cortical region (thalamus, caudate, putamen, pallidum, hippocampus, amygdala and accumbens), Cin; cingulate, Fro; frontal, Tem; temporal, Par; parietal, Occ; occipital. Data are presented as mean ± SD; * $p < 0.05$ one-way ANOVA with post-hoc Tukey tests.

The 3D brain surface projection of the kinetic analysis (K) was generated using the pixel-wise kinetic modeling tool (PXMOD). Parametric images (K pixel-wise) were adapted to the Montreal Neurological Institute (MNI) standard coordinate space and obtained using the 3D surface projection tool of the MIMvista medical program 6.4 (MIM Software Inc., Cleveland, OH, USA).

Segmentation of regional brain volume and measurement of cortical thickness were determined using surface-based analysis software (Freesurfer, version 5.3.0) (Du et al., 2007; Lacalle-Aurioles et al., 2014). Regional brain volume normalization was performed by linear regression against intracranial volumes (Hansen et al., 2015).

2.4. Statistical analysis

Data are presented as mean $\pm$ SD. Differences between groups were assessed by a one-way ANOVA with post-hoc Tukey tests for multiple comparisons and contrast analysis. Levene's test was performed to assess homogeneity of variances. All statistical analyses were carried out using SPSS 24.0 software (SPSS Inc., Chicago, IL, USA). Pearson correlations were performed to assess associations between K, CMR and plasma glucose or acetoacetate.

3. Results

3.1. Anthropomorphic data

The three groups did not differ significantly in age (74 ± 6 years), male to female ratio (2/3), body mass index (BMI) (26 ± 3), or blood parameters (Table 1). The Mini-Mental State Examination (MMSE) results were consistent with the clinical diagnosis of MCI or AD.

3.2. PET and MRI data

3.2.1. Kinetic analysis of brain glucose and ketone uptake

K_{Glu} and CMR_{Glu} were both significantly (~11%, [9–12%]) lower for the whole brain and major cortical regions (frontal, temporal, parietal and cingulate) in AD compared to CTL (Fig. 1), but no significant differences were noted between CTL and AD or MCI for the cerebellum, white matter or occipital lobes. K_{Glu} but not CMR_{Glu} was also lower in the subcortical regions in AD versus CTL. The cingulate was the only region with significantly lower K_{Glu} (~7%) and lower CMR_{Glu} in MCI compared to CTL. Due to brain atrophy, CMR_{Glu} calculated by region (not by 100 g of brain tissue) was significantly lower for the subcortical, frontal, temporal and parietal regions in AD compared to CTL (Fig. 2A). As a % of CMR_{Glu} in whole brain gray matter only, regional CMR_{Glu} was significantly lower in the temporal lobe in AD compared to CTL. A higher % of global CMR_{Glu} was observed in the parietal and occipital lobes in MCI compared to CTL and in the occipital lobe in AD compared to CTL (Fig. 2B).

Global K_{AcAc} and CMR_{AcAc} were not significantly different between the three groups, nor was CMR_{AcAc} different by region (Figs. 3–5). As a % of overall CMR_{AcAc} in gray matter, CMR_{AcAc} was significantly higher in the parietal and occipital lobes in MCI compared to CTL and higher in the occipital lobe in AD compared to CTL (Fig. 4B).

In all three groups combined, there was no significant correlation between blood glucose and CMR_{Glu}, but K_{Glu} was significantly negatively correlated to blood glucose ($r = -0.54$; $p < 0.0001$), a relationship that was progressively less significant in moving from CTL ($r = -0.68$; $p = 0.0002$), to MCI ($r = -0.56$; $p = 0.01$) to AD ($r = -0.38$; $p = 0.11$). Across all three groups combined, blood AcAc and CMR_{AcAc} were significantly positively correlated (r $= +0.80$; $p < 0.001$), a relationship that remained when
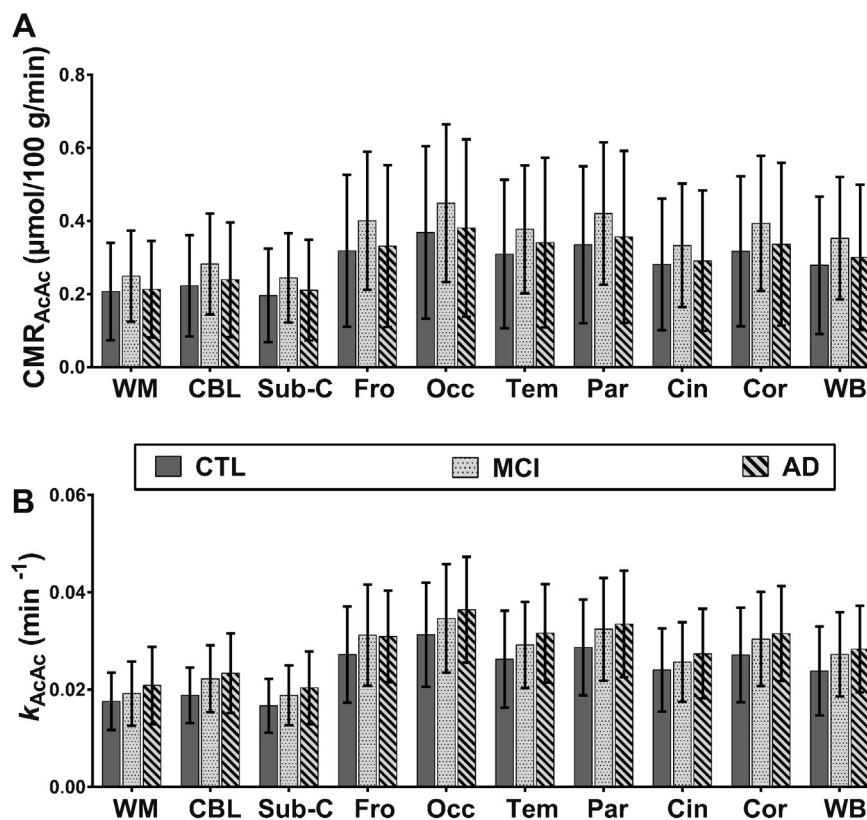

Fig. 3. Regional and whole brain ketone (^{11}C-acetoacetate) uptake in healthy older controls (CTL; $n = 24$), mild cognitive impairment (MCI; $n = 20$) and early Alzheimer's disease (AD; $n = 19$). **A**: Regional cerebral metabolic rate of acetoacetate per unit of brain tissue (CMR_{AcAc}). **B**: Regional constant rate uptake (K_{AcAc}). WM; white-matter, CBL; cerebellum, Sub–C; sub-cortical region (thalamus, caudate, putamen, pallidum, hippocampus, amygdala and accumbens), Fro; frontal, Occ; occipital, Tem; temporal, Par; parietal, Cin; cingulate, Cor; cortex, WB; whole brain. Data are presented as mean $\pm$ SD; * $p < 0.05$ ANOVA one-way with post-hoc Tukey tests.
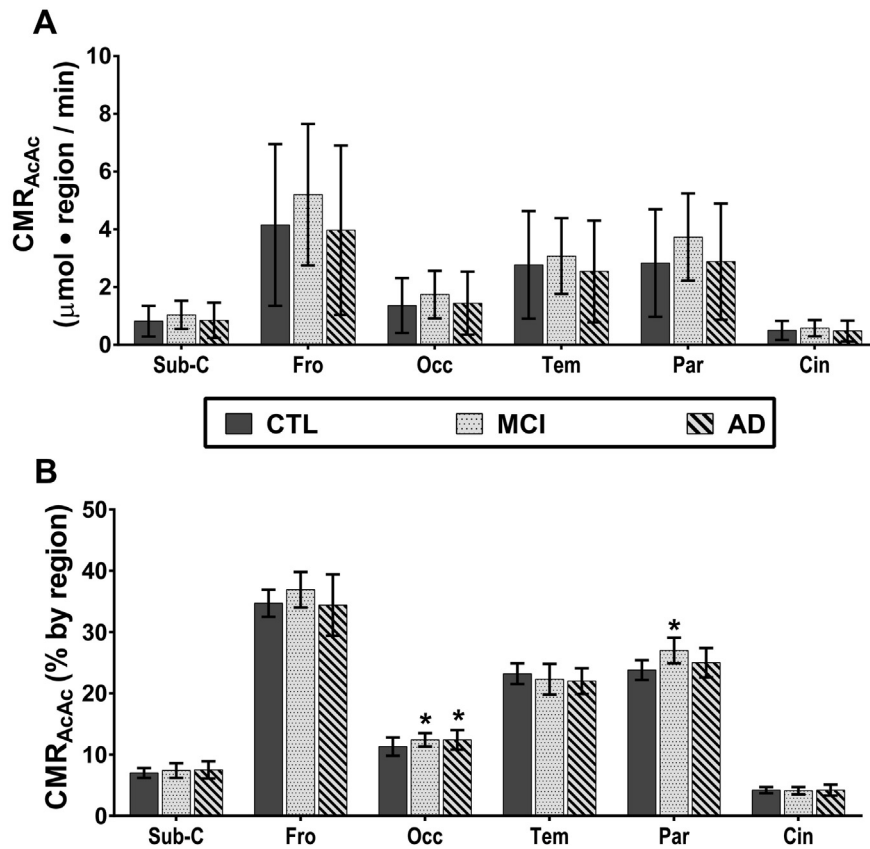
Fig. 4. Regional (^{11}C-acetoacetate) uptake in healthy older controls (CTL; $n = 24$), mild cognitive impairment (MCI; $n = 20$) and early Alzheimer's disease (AD; $n = 19$). **A:** Cerebral metabolic rate of glucose (CMR_{AcAc}) by major anatomical brain region. **B:** Percentage CMR_{AcAc} by region. Sub-C; sub-cortical region (thalamus, caudate, putamen, pallidum, hippocampus, amygdala and accumbens), Cin; cingulate, Fro; frontal, Tem; temporal, Par; parietal, Occ; occipital. Data are presented as mean $\pm$ SD; * $p < 0.05$ one-way ANOVA with post-hoc Tukey tests.

the three groups were analysed separately; CTL ($r = +0.81$; $p < 0.0001$), MCI ($r = +0.71$; $p = 0.0004$) and AD ($r = +0.87$; $p < 0.0001$) (Fig. 6).

3.2.2. Cortical volume and thickness

The volume of the cortex as a whole, the temporal lobe separately, and the subcortical regions grouped together (caudate, putamen, pallidum, hippocampus, amygdala and accumbens) was significantly lower by about 9%, 19%, and 8%, respectively, in AD versus CTL (Fig. 7). The temporal region as a whole and the hippocampus were also 11% smaller in MCI versus CTL. In MCI and AD versus CTL, cortical thickness was about 12% and 16% lower, respectively, in the regions with lower brain volume, as well as in the cingulate gyrus (isthmus, caudal anterior, posterior and rostral anterior).
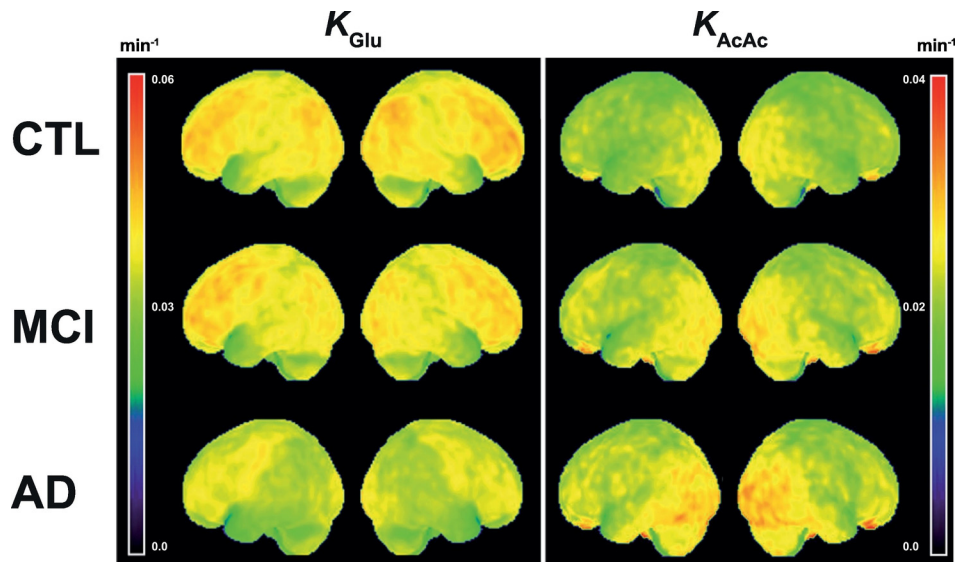

Fig. 5. Voxel-wise 3D surface projection of the brain uptake rate constant for glucose (K_{Glu}; min^{-1}) and acetoacetate (K_{AcAc}; min^{-1}) in healthy older controls (CTL; $n = 24$), mild cognitive impairment (MCI; $n = 20$) and early Alzheimer's disease (AD; $n = 19$).

Compared to CTL, CMR_{Glu}, K_{Glu}, brain volume and cortical thickness were all lower in the frontal lobes (lateral orbitofrontal, medial orbitofrontal) and temporal lobes (entorhinal, inferior temporal, middle temporal, superior temporal and temporal pole) of the AD group (Table 2 and Fig. 3). CMR_{Glu} and K_{Glu} were also about 18%, 10%, 12% and 9% lower, respectively, in the caudate, precuneus, isthmus of the cingulate and in the posterior cingulate in the MCI versus CTL group. K_{Glu} was significantly lower in the medial orbitofrontal cortex, the rostral anterior cingulate and the transverse temporal regions of the MCI versus CTL group.

4. Discussion

We report here a detailed comparison of regional brain AcAc and glucose uptake in cognitively healthy older people, MCI and early AD who were all relatively well-matched and in relatively similar and good metabolic control. We confirm the well-known brain glucose hypometabolism, regional brain atrophy and cortical thinning in MCI and AD (Mosconi et al., 2008; Osorio et al., 2010). The observed brain atrophy and reduction in cortical thickness in AD are in line with the literature which shows an initial reduction in the medial temporal lobe, extending to the cingulate and precuneus to finally the parietal, temporal and frontal regions (Verclytte et al., 2016). In AD, the glucose hypometabolism pattern was most apparent in the parietal and temporal lobes, posterior cingulate, and in the medial temporal and frontal regions.

CMR_{Glu} is traditionally expressed per 100 g of brain tissue but, given that the brain atrophies with age and more so in AD, we also report here CMR by anatomical region, both quantitatively and as a % of total brain CMR_{Glu}. This conversion of CMR to an anatomically-defined regional measure from a unit of tissue measure demonstrates that it was essentially equivalent to the traditional CMR_{Glu} per 100 g of tissue because of the relatively mild brain atrophy at the early stage of AD.

In MCI, lower ^{18}F–FDG uptake is commonly reported for the posterior cingulate and also for the hippocampus and/or the precuneus (Bailly et al., 2015; Del Sole et al., 2008; Minoshima et al., 1997; Mosconi et al., 2005; Mosconi et al., 2008). The posterior cingulate seem to be a common point of agreement, but the medial temporal region, including the hippocampus, entorhinal cortex and the precuneus can be affected in MCI depending on age of onset, amnestic presentation, impairment in single or multiple cognitive domains or other factors (Petersen, 2004). Our observation of higher gray matter % CMR_{Glu} in the parietal lobe as a whole in the MCI group (Fig. 2) could be associated with the brain hyperactivation that is also reported in MCI (Ashraf et al., 2015). The increase in % CMR_{Glu} localized to the parietal lobe in MCI was only apparent when the CMR_{Glu} was expressed per brain region and not per 100 g of brain tissue, i.e. was more a function of atrophy of this region rather than reduced glucose metabolism per unit of brain tissue in the parietal lobe. Higher CMR_{Glu} in the parietal lobe may reflect a compensatory response to the early stage of the disease (Ashraf et al., 2015) because it disappeared in those with early AD (Fig. 2B).

Our dual tracer sequential PET analysis demonstrated that there was a distinctly different pattern of brain $[^{11}C]$-AcAc compared to $[^{18}F]$-FDG metabolism in which the regional deterioration of brain glucose uptake (CMR_{Glu} and K_{Glu}) in MCI and AD was not observed for CMR_{AcAc}, CMR_{Ketone} or K_{AcAc}. Neither the greater variability of K_{AcAc} than for K_{Glu} nor the relatively low blood ketones were responsible for these similar brain ketone uptake values across the three groups. These results further support the hypothesis that the problem with brain fuel uptake in MCI and AD is specific to glucose and that rescue of brain energy
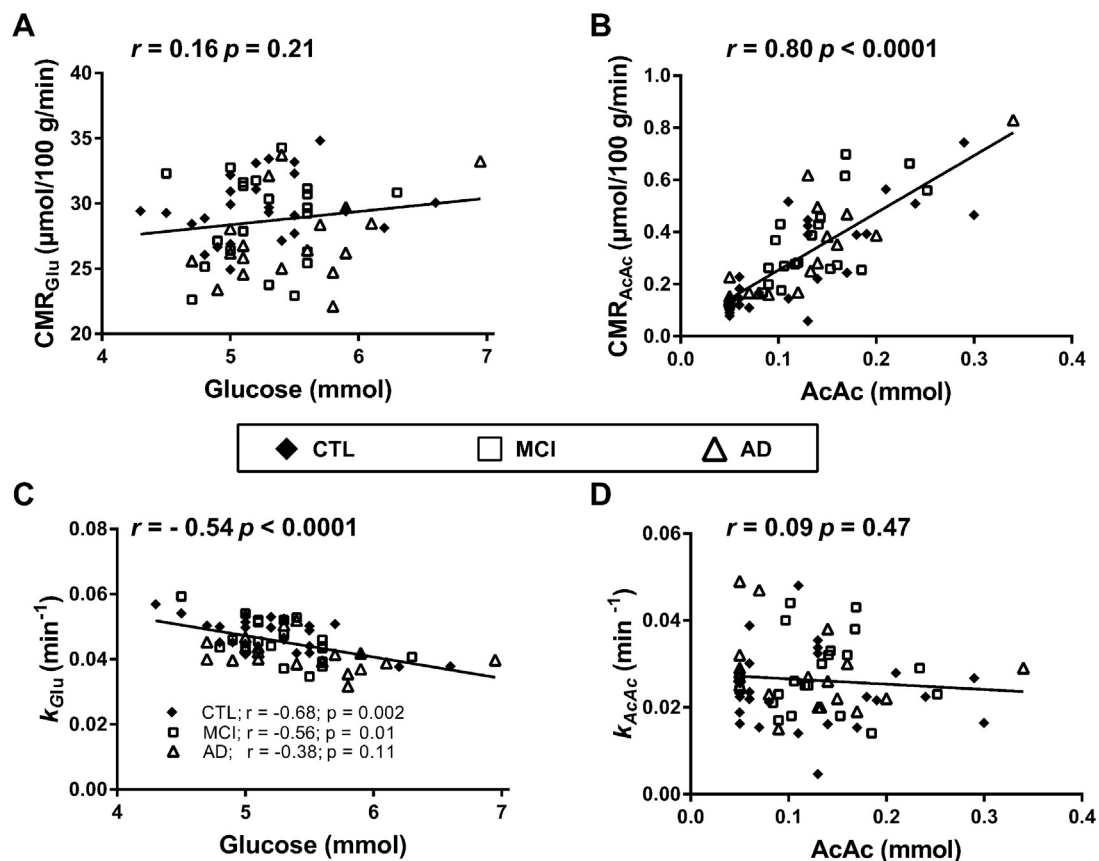

Fig. 6. Correlation between cerebral metabolic rate (CMR) or rate constant (K) and blood glucose (A, C) or acetoacetate (AcAc) (B, D) in healthy older controls (CTL; $n = 24$), mild cognitive impairment (MCI; $n = 20$) and early Alzheimer's disease (AD; $n = 19$).
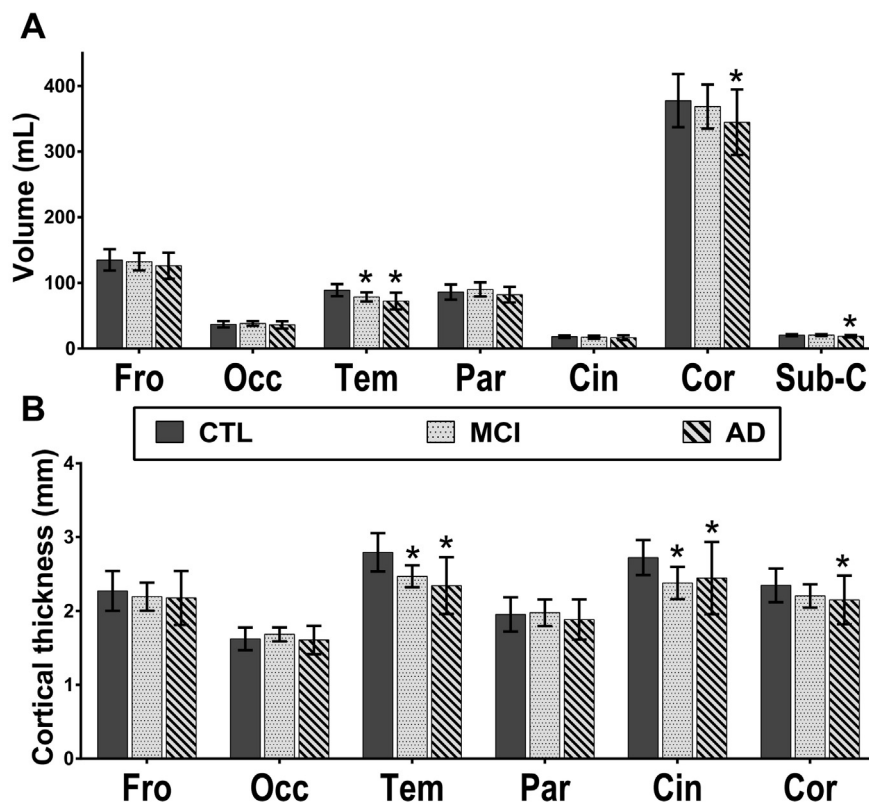
Fig. 7. Regional and whole brain volumes and cortical thickness in healthy older controls (CTL; $n = 24$), mild cognitive impairment (MCI; $n = 20$) and early Alzheimer's disease (AD; $n = 19$). **A**: Regional brain volumes. **B**: Regional brain cortical thickness. Fro; frontal, Occ; occipital, Tem; temporal, Par; parietal, Cin; cingulate, Cor; cortex, Sub–C; sub-cortical region (thalamus, caudate, putamen, pallidum, hippocampus, amygdala and accumbens). Data are presented as mean $\pm$ SD; * $p < 0.05$ one-way ANOVA with post-hoc Tukey tests.

metabolism using a ketogenic intervention is plausible and warranted further attention (Castellano et al., 2015; Castellano et al., 2017; Cunnane et al., 2016b).

We have shown that light-to-moderate physical exercise increases brain K_{AcAc} and CMR_{AcAc} by 2–3 fold (Castellano et al., 2017). Brain ketone PET also demonstrates that a ketogenic diet consumed for just four days is sufficient to raise brain ketone uptake by 6 fold (Courchesne-Loyer et al., 2016). Hence, our quantitative dual tracer PET method demonstrates that specifically brain ketone uptake but not brain glucose (FDG) can be increased by either a ketogenic intervention or by physical exercise, both of which may therefore be useful for brain energy rescue in AD.

A constraint of the quantitative PET method is that the [18F]-FDG image acquisition normally lasts 1 h, which can be challenging for compliance within the scanner, especially in older people. Shortening the scan to 30 min (starting 30 min post-tracer injection) results in less head motion during the imaging session, but also entails adjustments to blood sampling for the input function. For the first 30 min following the injection of [18F]-FDG, blood samples alone were used for the input function, whereas for the imaging session (30–60 min post-tracer injection), a blood-derived input function was used (Vriens et al., 2009). This approach matches more closely the AD neuroimaging initiative (ADNI) PET protocol (Jagust et al., 2010; Jagust et al., 2015).

The stronger inverse correlation we observed between K_{Glu} and blood glucose in the CTL group than in the MCI or AD groups requires further investigation to determine whether it has implications for the impact of insulin resistance on AD risk (Fig. 6). The significant positive correlation and similar slope of the relation between plasma AcAc and brain CMR_{AcAc} in all three groups confirms previous observations (Castellano et al., 2015; Castellano et al., 2017), and demonstrates that in MCI and early AD the brain can utilize ketones at the same rate as in healthy adults. Therefore, in MCI or AD, the brain should be able to utilize more ketones if they were available, for example, during

moderate nutritional ketosis induced with medium chain triglyceride (Vandenberghe et al., 2017).

Quantifying brain fuel metabolism (CMR) by brain region rather than by unit of brain tissue as is usually done provides insight into the relative distribution of glucose or ketones throughout the whole brain as well as the impact of increased level of brain atrophy on their utilization in MCI and AD. In all three groups, the ratio of the % CMR_{AcAc} over %CMR_{Glu} by region was somewhat higher in the temporal and occipital regions (non-significant) than in the other brain areas, indicating relatively higher ketone consumption in these two major anatomical brain areas compared to the rest of the brain in older people regardless of their cognitive status (Fig. 8). The skewed fuel utilization towards ketones in temporal cortex as a whole was significantly higher in the AD compared to CTL group (Fig. 8). This confirms that the relative deterioration in brain fuel utilization seen per unit of temporal cortical tissue (classic CMR_{Glu} units) is specific to glucose and suggests that a ketogenic intervention should be able to compensate for at least part of the glucose deficit in the temporal cortex in MCI and AD.

Table 2
Whole brain kinetics of [18F]-FDG and [11C]-AcAc, and brain gray matter volumes and cortical thickness in cognitively healthy older adults (CTL), mild cognitive impairment (MCI), and early Alzheimer disease (AD).

	CTL ($N = 24$)	MCI ($N = 20$)	AD ($N = 19$)
CMR_{Glu} (µmol/100 g/min)	29.7 ± 2.5	29.1 ± 3.2	27.0 ± 3.3*
K_{Glu} (min^{-1})	0.047 ± 0.005	0.045 ± 0.006	0.041 ± 0.005*
CMR_{AcAc} (µmol/100 g/min)	0.28 ± 0.19	0.35 ± 0.17	0.30 ± 0.20
K_{AcAc} (min^{-1})	0.024 ± 0.009	0.027 ± 0.009	0.028 ± 0.009
$CMR_{ketones}$ (µmol/100 g/min)	0.71 ± 0.51	0.96 ± 0.48	0.89 ± 0.62
Gray matter volume (mL)[a]	378 ± 40	369 ± 34	344 ± 50*
Cortical thickness (mm)	2.35 ± 0.23	2.20 ± 0.16	2.15 ± 0.33*

Cerebral metabolic rate; CMR, rate constant uptake; K, glucose;Glu, acetoacetate;AcAc. One-way ANOVA and Tukey's post hoc test * $p < 0.05$; [a] Cortex only.
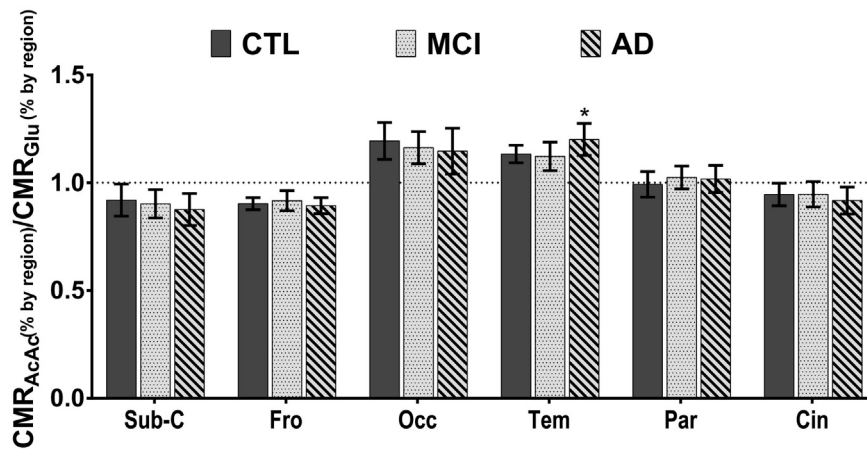
Fig. 8. Regional ratio of CMR_{AcAc} (% by region)/CMR_{Glu} (% by region) in healthy older controls (CTL; $n = 24$), mild cognitive impairment (MCI; $n = 20$) and early Alzheimer's disease (AD; $n = 19$) Sub-C; sub-cortical region (thalamus, caudate, putamen, pallidum, hippocampus, amygdala and accumbens), Fro; frontal, Occ; occipital, Tem; temporal, Par; parietal, Cin; cingulate. Data are presented as mean $\pm$ SD; * $p < 0.05$ one-way ANOVA with post-hoc Tukey tests.

5. Conclusions

This cross-sectional study shows that despite widespread brain glucose hypometabolism, brain atrophy and cortical thinning, basal brain ketone uptake remains normal in MCI and AD. Hence, brain energy deprivation in AD clearly appears to be specific to glucose and is a function of defective brain uptake and utilization of glucose not to lower brain glucose availability per se. The deficit in brain glucose utilization was more highly regionalized in AD and especially in MCI than were the structural changes which were widespread. These results support the need to assess whether providing more of the brain's main alternative fuel, ketones, would result in a similar increase in CMR_{Ket} as seen in younger adults (Courchesne-Loyer et al., 2016). If so, assessing whether ketogenic interventions that sufficiently compensate for the brain energy deficit could be beneficial for cognitive symptoms in MCI or AD would be warranted.

Conflict of interest

References

Ashraf, A., Fan, Z., Brooks, D.J., Edison, P., 2015. Cortical hypermetabolism in MCI subjects: a compensatory mechanism? Eur. J. Nucl. Med. Mol. Imaging 42, 447–458.

Bailly, M., Destrieux, C., Hommet, C., Mondon, K., Cottier, J.P., Beaufils, E., Vierron, E., Vercouillie, J., Ibazizene, M., Voisin, T., Payoux, P., Barre, L., Camus, V., Guilloteau, D., Ribeiro, M.J., 2015. Precuneus and cingulate cortex atrophy and Hypometabolism in patients with Alzheimer's disease and mild cognitive impairment: MRI and (18)F-FDG PET quantitative analysis using FreeSurfer. Biomed. Res. Int. 583931, 2015.

Blomqvist, G., Thorell, J.O., Ingvar, M., Grill, V., Widen, L., Stone-Elander, S., 1995. Use of R-beta-[1-11C]hydroxybutyrate in PET studies of regional cerebral uptake of ketone bodies in humans. Am. J. Physiol. 269, E948–E959.

Brown, R.K., Bohnen, N.I., Wong, K.K., Minoshima, S., Frey, K.A., 2014. Brain PET in suspected dementia: patterns of altered FDG metabolism. Radiographics 34, 684–701.

Cahill Jr., G.F., 2006. Fuel metabolism in starvation. Annu. Rev. Nutr. 26, 1–22.

Castellano, C.A., Nugent, S., Paquet, N., Tremblay, S., Bocti, C., Lacombe, G., Imbeault, H., Turcotte, E., Fulop, T., Cunnane, S.C., 2015. Lower brain 18F-fluorodeoxyglucose uptake but normal 11C-acetoacetate metabolism in mild Alzheimer's disease dementia. J. Alzheimers Dis. 43, 1343–1353.

Castellano, C.A., Paquet, N., Dionne, I.J., Imbeault, H., Langlois, F., Croteau, E., Tremblay, S., Fortier, M., Matte, J.J., Lacombe, G., Fulop, T., Bocti, C., Cunnane, S.C., 2017. A 3-Month aerobic training program improves brain energy metabolism in mild alzheimer's disease: preliminary results from a neuroimaging study. J. Alzheimers Dis.

Courchesne-Loyer, A., Fortier, M., Tremblay-Mercier, J., Chouinard-Watkins, R., Roy, M., Nugent, S., Castellano, C.A., Cunnane, S.C., 2013. Stimulation of mild, sustained ketonemia by medium-chain triacylglycerols in healthy humans: estimated potential contribution to brain energy metabolism. Nutrition 29, 635–640 (Burbank, Los Angeles County, Calif).

Courchesne-Loyer, A., Croteau, E., Castellano, C.A., St-Pierre, V., Hennebelle, M., Cunnane, S.C., 2016. Inverse relationship between brain glucose and ketone metabolism in adults during short-term moderate dietary ketosis: a dual tracer quantitative positron emission tomography study. J Cereb Blood Flow Metab.

Cunnane, S.C., Courchesne-Loyer, A., St-Pierre, V., Vandenberghe, C., Pierotti, T., Fortier, M., Croteau, E., Castellano, C.A., 2016a. Can ketones compensate for deteriorating brain glucose uptake during aging? Ann. N. Y. Acad. Sci. 1367, 12–20.

Cunnane, S.C., Courchesne-Loyer, A., Vandenberghe, C., St-Pierre, V., Fortier, M., Hennebelle, M., Croteau, E., Bocti, C., Fulop, T., Castellano, C.A., 2016b. Can ketones help rescue brain fuel supply in later life? Implications for cognitive health during aging and the treatment of Alzheimer's disease. Front. Mol. Neurosci. 9, 53.

Del Sole, A., Clerici, F., Chiti, A., Lecchi, M., Mariani, C., Maggiore, L., Mosconi, L., Lucignani, G., 2008. Individual cerebral metabolic deficits in Alzheimer's disease and amnestic mild cognitive impairment: an FDG PET study. Eur. J. Nucl. Med. Mol. Imaging 35, 1357–1366.

Du, A.T., Schuff, N., Kramer, J.H., Rosen, H.J., Gorno-Tempini, M.L., Rankin, K., Miller, B.L., Weiner, M.W., 2007. Different regional patterns of cortical thinning in Alzheimer's disease and frontotemporal dementia. Brain 130, 1159–1166.

Dukart, J., Kherif, F., Mueller, K., Adaszewski, S., Schroeter, M.L., Frackowiak, R.S., Draganski, B., 2013. Generative FDG-PET and MRI model of aging and disease progression in Alzheimer's disease. PLoS Comput. Biol. 9, e1002987.

Gauthier, S., Reisberg, B., Zaudig, M., Petersen, R.C., Ritchie, K., Broich, K., Belleville, S., Brodaty, H., Bennett, D., Chertkow, H., Cummings, J.L., de Leon, M., Feldman, H., Ganguli, M., Hampel, H., Scheltens, P., Tierney, M.C., Whitehouse, P., Winblad, B., 2006. Mild cognitive impairment. Lancet 367, 1262–1270.

Hansen, T.I., Brezova, V., Eikenes, L., Haberg, A., Vangberg, T.R., 2015. How does the accuracy of intracranial volume measurements affect normalized brain volumes? Sample size estimates based on 966 subjects from the HUNT MRI cohort. AJNR Am. J. Neuroradiol. 36, 1450–1456.

Hebert, R., Carrier, R., Bilodeau, A., 1988. The functional autonomy measurement system (SMAF): description and validation of an instrument for the measurement of handicaps. Age Ageing 17, 293–302.

Jagust, W.J., Bandy, D., Chen, K., Foster, N.L., Landau, S.M., Mathis, C.A., Price, J.C., Reiman, E.M., Skovronsky, D., Koeppe, R.A., 2010. The Alzheimer's disease neuroimaging initiative positron emission tomography core. Alzheimers Dement. 6, 221–229.

Jagust, W.J., Landau, S.M., Koeppe, R.A., Reiman, E.M., Chen, K., Mathis, C.A., Price, J.C., Foster, N.L., Wang, A.Y., 2015. The Alzheimer's disease neuroimaging initiative 2 PET Core: 2015. Alzheimers Dement. 11, 757–771.

Jicha, G.A., Abner, E., Schmitt, F.A., Cooper, G.E., Stiles, N., Hamon, R., Carr, S., Smith, C.D., Markesbery, W.R., 2008. Clinical features of mild cognitive impairment differ in the research and tertiary clinic settings. Dement. Geriatr. Cogn. Disord. 26, 187–192.

Lacalle-Aurioles, M., Mateos-Perez, J.M., Guzman-De-Villoria, J.A., Olazaran, J., Cruz-Orduna, I., Aleman-Gomez, Y., Martino, M.E., Desco, M., 2014. Cerebral blood flow is an earlier indicator of perfusion abnormalities than cerebral blood volume in Alzheimer's disease. J. Cereb. Blood Flow Metab. 34, 654–659.

Logan, J., 2000. Graphical analysis of PET data applied to reversible and irreversible tracers. Nucl. Med. Biol. 27, 661–670.

Lying-Tunell, U., Lindblad, B.S., Malmlund, H.O., Persson, B., 1981. Cerebral blood flow and metabolic rate of oxygen, glucose, lactate, pyruvate, ketone bodies and amino acids. Acta Neurol. Scand. 63, 337–350.

McKhann, G.M., Knopman, D.S., Chertkow, H., Hyman, B.T., Jack Jr., C.R., Kawas, C.H., Klunk, W.E., Koroshetz, W.J., Manly, J.J., Mayeux, R., Mohs, R.C., Morris, J.C., Rossor, M.N., Scheltens, P., Carrillo, M.C., Thies, B., Weintraub, S., Phelps, C.H., 2011. The diagnosis of dementia due to Alzheimer's disease: recommendations from the National Institute on Aging-Alzheimer's Association workgroups on diagnostic guidelines for Alzheimer's disease. Alzheimers Dement. 7, 263–269.

Minoshima, S., Giordani, B., Berent, S., Frey, K.A., Foster, N.L., Kuhl, D.E., 1997. Metabolic reduction in the posterior cingulate cortex in very early Alzheimer's disease. Ann. Neurol. 42, 85–94.

Mosconi, L., Tsui, W.H., De Santi, S., Li, J., Rusinek, H., Convit, A., Li, Y., Boppana, M., de Leon, M.J., 2005. Reduced hippocampal metabolism in MCI and AD: automated FDG-PET image analysis. Neurology 64, 1860–1867.

Mosconi, L., Tsui, W.H., Herholz, K., Pupi, A., Drzezga, A., Lucignani, G., Reiman, E.M., Holthoff, V., Kalbe, E., Sorbi, S., Diehl-Schmid, J., Perneczky, R., Clerici, F., Caselli, R., Beuthien-Baumann, B., Kurz, A., Minoshima, S., de Leon, M.J., 2008. Multicenter standardized 18F-FDG PET diagnosis of mild cognitive impairment, Alzheimer's disease, and other dementias. J. Nucl. Med. 49, 390–398.

Mosconi, L., Mistur, R., Switalski, R., Tsui, W.H., Glodzik, L., Li, Y., Pirraglia, E., De Santi, S., Reisberg, B., Wisniewski, T., de Leon, M.J., 2009. FDG-PET changes in brain glucose metabolism from normal cognition to pathologically verified Alzheimer's disease. Eur. J. Nucl. Med. Mol. Imaging 36, 811–822.

Nugent, S., Tremblay, S., Chen, K.W., Ayutyanont, N., Roontiva, A., Castellano, C.A., Fortier, M., Roy, M., Courchesne-Loyer, A., Bocti, C., Lepage, M., Turcotte, E., Fulop, T., Reiman, E.M., Cunnane, S.C., 2014. Brain glucose and acetoacetate metabolism: a comparison of young and older adults. Neurobiol. Aging 35, 1386–1395.

Ogawa, M., Fukuyama, H., Ouchi, Y., Yamauchi, H., Kimura, J., 1996. Altered energy metabolism in Alzheimer's disease. J. Neurol. Sci. 139, 78–82.

Osorio, R.S., Berti, V., Mosconi, L., Li, Y., Glodzik, L., De Santi, S., de Leon, M.J., 2010. Evaluation of Early Dementia (Mild Cognitive Impairment). PET Clin. 5, pp. 15–31.

Pagani, M., De Carli, F., Morbelli, S., Oberg, J., Chincarini, A., Frisoni, G.B., Galluzzi, S., Perneczky, R., Drzezga, A., van Berckel, B.N., Ossenkoppele, R., Didic, M., Guedj, E., Brugnolo, A., Picco, A., Arnaldi, D., Ferrara, M., Buschiazzo, A., Sambuceti, G., Nobili, F., 2015. Volume of interest-based [18F]fluorodeoxyglucose PET discriminates MCI converting to Alzheimer's disease from healthy controls. A European Alzheimer's disease consortium (EADC) study. Neuroimage Clin. 7, pp. 34–42.

Petersen, R.C., 2004. Mild cognitive impairment as a diagnostic entity. J. Intern. Med. 256, 183–194.

Pfefferbaum, A., Rohlfing, T., Rosenbloom, M.J., Sullivan, E.V., 2012. Combining atlas-based parcellation of regional brain data acquired across scanners at 1.5 T and 3.0 T field strengths. Neuroimage 60, 940–951.

Vandenberghe, C., St-Pierre, V., Pierotti, T., Fortier, M., Castellano, C.A., Cunnane, S.C., 2017. Tricaprylin alone increases plasma ketone response more than coconut oil or other medium-chain triglycerides: an acute crossover study in healthy adults. Current developments in nutrition. 1, pp. 1–5.

Verclytte, S., Lopes, R., Lenfant, P., Rollin, A., Semah, F., Leclerc, X., Pasquier, F., Delmaire, C., 2016. Cerebral Hypoperfusion and Hypometabolism detected by arterial spin labeling MRI and FDG-PET in early-onset Alzheimer's disease. J. Neuroimaging 26, 207–212.

Vriens, D., de Geus-Oei, L.F., Oyen, W.J., Visser, E.P., 2009. A curve-fitting approach to estimate the arterial plasma input function for the assessment of glucose metabolic rate and response to treatment. J. Nucl. Med. 50, 1933–1939.